

Investigation of electrical contact resistance for nonconductive film functionalized with π -conjugated self-assembled molecules

Hai Dong, Yi Li, Myung Jin Yim, Kyung Sik Moon, and C. P. Wong^{a)}

School of Materials Science and Engineering, Georgia Institute of Technology,
771 Ferst Drive, Atlanta, Georgia 30332-0245

(Received 7 December 2006; accepted 23 January 2007; published online 26 February 2007)

Nonconductive adhesive/nonconductive film (NCA/NCF) bonding technology has attracted increasing research interests as lead-free interconnect. During bonding, heat and pressure are applied and the direct physical contacts between the two surfaces of integrated circuit bump and substrate bond pad can be achieved. The electrical contact resistance of a NCA/NCF joint is controlled by the pressure, roughness and NCA/NCF material properties. An accurate prediction of contact resistance can help guide experiment setup towards improving the electrical performance of NCA/NCF. In this study, a model is developed and correlated to experiments. The effects of NCA/NCF material properties on electrical contact resistance are investigated. © 2007 American Institute of Physics. [DOI: 10.1063/1.2709638]

Although the electronics industry has made considerable advances over the past few decades, the essential requirements of interconnects among all types of components in all electronic and photonic systems remain unchanged. They need to be electrically connected for power, ground, and signal transmissions, where tin/lead (Sn/Pb) solder alloy has been the *de facto* interconnect material in most areas of electronic packaging. These include interconnection technologies such as surface mount technique, ball grid array, chip scale package, and flip chip technology. However, there are increasing concerns nowadays with the use of tin-lead alloy solders, since tin-lead solders contain lead, a material hazardous to human and the environment. In response to concerns for the environment and human health, some legislations and restriction of banning lead from electronic products have been introduced in many countries around the world. As such, major electronic manufacturers have stepped up their search for alternatives to lead-containing solders.

Polymer-based conductive adhesives have drawn much attention as an environmentally friendly solution for lead-free interconnects.¹ In addition to electronic conductive adhesives, nonconductive adhesive/nonconductive film (NCA/NCF) bonding technology is one of the lead-free options,²⁻⁴ which requires no conductive fillers and a relatively high bonding pressure to enable bonding between the integrated circuit (IC) chip and the substrate coupled with heat. During bonding, the heat and pressure are applied simultaneously for some time, and the direct physical contact between the two surfaces of the IC bump and the substrate bond pad can be made. A permanent joint is then formed by NCA/NCF resin curing/solidification. As shown in Fig. 1, physical contacts by the rough structure of the bottom and top pad surfaces lead to the electrical conduction between the two pads. To accomplish a joint with acceptable electrical contact resistance, relatively high pressure (200 MPa) and high shrinkage polymer resin are required.

Compared to other bonding techniques, conductive joints with NCA/NCFs provide a number of advantages such as no short circuiting and fine pitch. In fact, the pitch size of

the NCA/NCF joints can be limited only by the pitch pattern of the bond pad, rather than the adhesive materials. However, since the electrical conductivity of NCA/NCF is achieved through physical/mechanical contact and no metallurgical joints are formed, it has limited electrical conductance and current carrying capability. In this study, a micromechanical model will be developed to predict the electrical performance and applied to guide material development for better electrical performance. The effects of NCA/NCF material properties on electrical contact resistance will be investigated.

The experimental investigation of Williamson *et al.* established that many of the manufacturing processes produce surfaces with an isotropic Gaussian distribution of heights of the surface asperities.⁵ In most analyses of the microcontact involving two rough Gaussian surfaces, the analysis can be simplified by considering the contact between a single surface (with effective surface roughness characteristics) and a perfectly flat surface. The equivalent root mean square (rms) roughness σ and the equivalent mean absolute surface slope m are, respectively, defined as

$$\sigma = \sqrt{\sigma_1^2 + \sigma_2^2}, \quad (1)$$

$$m = \sqrt{m_1^2 + m_2^2}, \quad (2)$$

where subscripts 1 and 2 are used to denote the two contacting bodies.

The number of contacts between two surfaces follows from the approach of Cooper *et al.*,⁶

$$n_s = \frac{1}{16} \left(\frac{m}{\sigma} \right)^2 \frac{\exp(-Y^2/\sigma^2)}{\operatorname{erf}(Y/\sqrt{2}\sigma)} A_a, \quad (3)$$

where A_a is the area of apparent contact of a NCA/NCF joint and Y is the mean-planes separation of the contacting surfaces. For conforming rough surfaces at which the asperities undergo plastic deformation, Cooper *et al.* showed that the mean-planes separation Y can be written as

^{a)}Fax: 404-894-9140. Electronic mail: cp.wong@mse.gatech.edu

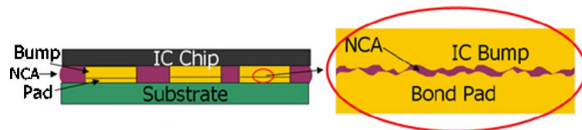


FIG. 1. (Color online) Schematic illustration of a NCA/NCF joint.

$$Y = \sqrt{2}\sigma \operatorname{erfc}^{-1}\left(\frac{2P}{H_{\text{mic}}}\right), \quad (4)$$

where $P = F/A_n$, which is the applied pressure (A_n is the area normal to the applied force and in our case A_n is equal to A_a), and H_{mic} is the microhardness of the softer surface in contact.

The average radius of an elastoplastic physical contact can be expressed as

$$a = \sqrt{8/\pi}(\sigma/m)\exp(\lambda^2)\operatorname{erfc}(\lambda), \quad (5)$$

where $\lambda = Y/\sqrt{2}\sigma$.

From these equations, one can calculate the contact area and number of contacts based on the surface roughness, material hardness, and applied external pressure.

In order to obtain the electrical resistance of a NCA/NCF joint, one needs to determine the resistance of a physical contact first. For a microcontact, the contact resistance is composed of constriction and tunnel resistance.⁷ Constriction resistance occurs as the electrical current must squeeze through the asperities to cross the interface. Tunnel resistance is due to the intermediate layer between the metal surfaces. The total resistance of a physical contact can be written as

$$R = R_c + R_t = (\rho_1/4a + \rho_2/4a) + \xi/\pi a^2, \quad (6)$$

where R_c is the constriction resistance, R_t is the tunnel resistance, ρ_1 and ρ_2 are the bulk electrical resistivities of the two contacting bodies, a is the radius of contact area, and ξ is the tunnel resistivity of the interface.

As mentioned before, tunnel resistance is due to the intermediate layer between the metal surfaces. The intermediate layer may consist of a thin film of NCA/NCF material. Tunnel resistivity is a function of the film thickness s , the work function ϕ for electron emission from metal into film (electron-injection barrier), and the relative permittivity ϵ_r of the material of the film. It can be expressed as⁷

$$\xi = 0.5 \times 10^{-12} \frac{A^2 \exp(AB)}{1 + AB} \quad (\Omega \text{ cm}^2), \quad (7)$$

where $A = 7.32(s - 7.2/\phi)$ and $B = 0.1265\sqrt{\phi - (10/s\epsilon_r)}$, with ϕ in eV and s in angstrom.

Based on Eq. (6), the electrical resistance of a NCA/NCF joint can be written as follows by assuming that all physical contacts have an average contact area:

$$R_{\text{joint}} = R/n_s = [(\rho_1/4a + \rho_2/4a) + \xi/\pi a^2]/n_s, \quad (8)$$

where n_s is the number of physical contacts of a NCA/NCF joint, as in Eq. (3). Based on the above derivation, one can tell that the contact resistance of a NCA/NCF joint is dependent on surface morphology, processing pressure, and material properties. Among these parameters, the intermediate film thickness is the most difficult to identify. Therefore, experiments were conducted to obtain the film thickness, and then the effect of the material properties can be investigated.

The NCF base formulation was prepared with epoxy, curing agent, and silane coupling agents. The NCF was prebonded on the Au-finished substrate at 80 °C for 5 s. After removal of separator film, the substrate was aligned and the final bonding of NCF was conducted at 150 °C for 40 min with the application of bonding pressure at 300 MPa. The electrical resistance and current carrying capability of the NCF joints (contact area: $100 \times 100 \mu\text{m}^2$) on Au-finished test vehicle was measured by a four-point probe method. Based on our measurement, the total resistance of a NCA/NCF joint is $1.5 \times 10^{-4} \Omega$.

Atomic force microscopy was applied to study the surface roughness of the gold pad used in our experiment. Based on the measurement, the rms roughness σ equaled to 820 nm, and the mean absolute surface slope m equaled to 0.27. From the literature, the microhardness of gold was identified as 1386 MPa.⁸ The bulk electrical resistivity for gold is $0.0452 \Omega \text{ nm}$, and the applied pressure is 300 MPa. By substituting these values to Eqs. (3) and (5), one can obtain n_s as 36 and a as 2850 nm. Therefore, the constriction resistance of a microcontact is equal to $0.0452/(2 \times 2850)$, which is $7.93 \times 10^{-6} \Omega$. The total constriction resistance of all microcontacts on the NCF joint is equal to $7.93 \times 10^{-6}/n_s$, which is $2.20 \times 10^{-7} \Omega$.

Based on our measurement, the total resistance of a NCA/NCF joint is $1.5 \times 10^{-4} \Omega$. As one can see, the constriction resistance only composed a negligible amount of a NCA/NCF joint resistance. Therefore, our micromechanical model showed that the tunnel resistance is the main source for the joint resistance. Now the electrical resistance of a NCA/NCF joint can be written as

$$R_{\text{joint}} = (\xi/\pi a^2)/n_s. \quad (9)$$

From Eq. (9), one can obtain the tunnel resistivity (ξ) as $1.40 \times 10^{-9} \Omega \text{ cm}^2$ for our experiment. In order to increase the performance of the NCA/NCF material, one needs to decrease the tunnel resistivity. From Eq. (7) one can tell that the tunnel resistivity is dependent on the film thickness, electron-injection barrier, and dielectric constant of the intermediate layer material. The thickness of the film is dependent on the applied processing pressure and it cannot be increased further due to process requirement. The parameters one can control are electron-injection barrier and dielectric constant.

Before we can investigate the effect of electron-injection barrier and dielectric constant, the NCA/NCF film thickness between the two gold pad surfaces needs to be estimated for our experiment, which can be fitted from Eq. (7). We already know that the tunnel resistivity (ξ) is equal to $1.40 \times 10^{-9} \Omega \text{ cm}^2$, and the dielectric constant of the base epoxy resin is about 3.5. The electron-injection barrier of electron from gold to intermediate film is difficult to measure. Based on the literature the work function of gold is 5.20 eV,⁹ while the electron affinity (EA) of the epoxy polymer (difference between lowest unoccupied molecular orbital and vacuum level) can be roughly taken as 2.5 eV. Then the 2.7 eV difference between the work function and EA gives the electron-injection barrier. By substituting these values into Eq. (7) one can obtain the film thickness as 5.3 Å. Since this film thickness is just an estimate, the effect of electron-injection barrier and dielectric constant will be investigated at different film thicknesses from 4.3 to 6.3 Å.

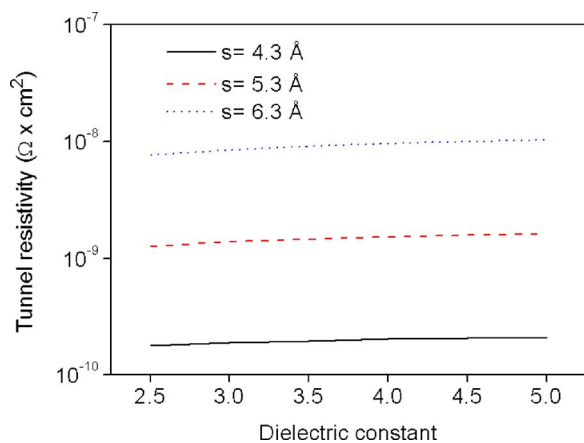


FIG. 2. (Color online) Effect of dielectric constant on tunnel resistivity (electron-injection barrier=2.7 eV).

Figures 2 and 3 were calculated based on Eq. (7). Figure 2 shows the effect of film dielectric constant on tunnel resistivity at different film thicknesses. The electron-injection barrier is 2.7 eV. As one can tell tunnel resistivity remains almost unchanged when the dielectric constant is changed from 2.5 to 5. However, the effect of electron-injection barrier is much more significant. As one can see from Fig. 3, the tunnel resistivity decreased with the decreasing of electron-injection barrier. For all film thicknesses, the tunnel resistivity was reduced by two magnitudes when the electron-injection barrier was changed from 3.5 to 1.5 eV. Therefore, we think there is not much one can do in order to improve the electrical performance by modifying the dielectric property of the resin system. More researches should be conducted to reduce the tunnel resistivity by decreasing the electron-injection barrier.

π -conjugated self-assembled molecules have been studied in tuning the electron-injection barrier and electrical conduction of metal-molecule contact.¹⁰ In particular, conjugated molecules which have smaller gaps between the

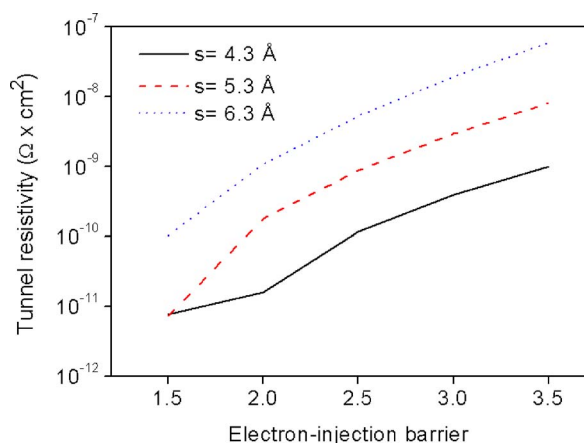


FIG. 3. (Color online) Effect of electron-injection barrier on tunnel resistivity (dielectric constant=3.5).

highest occupied molecular orbital and the lowest unoccupied molecular orbital and possess delocalized π electrons can contribute to conduction. Heimel *et al.* demonstrated that biphenyldithiol (BPD) can reduce the work function of gold by 1.02 eV.⁹

Based on our micromechanical model, electron-injection barrier plays an important role in controlling the tunnel resistivity of the interface. In order to improve the electrical conductivity of the NCA/NCF joint, BPD molecules are *in situ* mixed with NCA/NCF base formulation with a loading of 0.5 wt %. Following the same experimental steps described above, the electrical resistance of the NCF joints (contact area: $100 \times 100 \mu\text{m}^2$) is measured as $5 \times 10^{-5} \Omega$. Compared to an electrical resistance of $1.5 \times 10^{-4} \Omega$ for base NCA/NCF formulation with no BPD, the *in situ* incorporation of BPD decreased the electrical resistivity by 2/3.

In conclusion, in this study a micromechanical model was developed to study the electrical conductance of NCA/NCF assembly. Analytical expressions were obtained for both constriction and tunnel resistance. Modeling results showed that the constriction resistance was negligible compared to tunnel resistance.

Tunnel resistance is dependent on the material properties (dielectric constant and electron-injection barrier) and the processing pressure. Model results demonstrated that the electron-injection barrier played a much more important role in controlling the tunnel resistivity, compared to the effect of dielectric constant.

BPD was selected to improve the electrical performance of NCA/NCF material, since it can decrease the electron-injection barrier between gold and the thin film of NCA/NCF. Experimental results showed that the *in situ* incorporation of BPD was able to reduce the contact resistance by 2/3.

Our preliminary work pointed a potential way of enhancing the electrical performance of NCA/NCF. More systematic research needs to be conducted in the future, in order to identify the best π -conjugated self-assembled molecules and fine-tune the processing conditions to achieve better electrical conductance and higher current carrying capabilities.

¹Y. Li, K. Moon, and C. P. Wong, *Science* **308**, 1419 (2005).

²H. Yu, S. G. Mhaisalkar, and E. H. Wong, *J. Mater. Res.* **20**, 1324 (2005).

³L. K. The, E. Anto, C. C. Wong, S. G. Mhaisalkar, E. H. Wong, P. S. Teo, and Z. Chen, *Thin Solid Films* **462**, 446 (2004).

⁴M.-J. Yim, J.-S. Hwang, W. Kwon, K. W. Jang, and K.-W. Paik, *IEEE Trans. Electron. Packag. Manuf.* **26-2**, 150 (2003).

⁵J. B. Williamson, J. Pullen, R. T. Hunt, and D. Leonard, *Surface Mechanics*, edited by F. F. Ling (ASME, New York, 1969), p. 24.

⁶M. G. Cooper, B. B. Mikic, and M. M. Yovanovich, *Int. J. Heat Mass Transfer* **12**, 279 (1969).

⁷R. Holm, *Electric Contacts, Theory and Application* (Springer-Verlag, New York, 1967), p. 123.

⁸B. Kshirsagar, P. Misra, N. Jampana, and M. V. Krishna Murthy, *J. Heat Transfer* **127**, 657 (2005).

⁹G. Heimel, L. Romaner, J.-L. Bredas, and E. Zojer, *Phys. Rev. Lett.* **96**, 196806 (2006).

¹⁰A. Kahn, N. Koch, and W. Gao, *J. Polym. Sci., Part B: Polym. Phys.* **41**, 2529 (2003).